Insertion of Alzheimer's Aβ40 Peptide into Lipid Monolayers

Canay Ege and Ka Yee C. Lee
Department of Chemistry, The Institute for Biophysical Dynamics, and the James Franck Institute, The University of Chicago, Chicago, Illinois

ABSTRACT The amyloid beta (Aβ) peptide is the major component found in the amyloid deposits in the brains of Alzheimer's disease patients. In vitro studies have demonstrated that the aggregation of Aβ can take place at three orders of magnitude lower concentrations in the presence of phospholipid molecules compared to bulk peptide studies, suggesting that membrane lipids may mediate Aβ toxicity. To understand the interaction of Aβ with lipid membranes, we have examined Aβ40 with anionic dipalmitoylphosphatidylglycerol (DPPG), zwitterionic dipalmitoylphosphatidylcholine (DPPC), and cationic dipalmitoyltrimethylammonium propane (DPTAP) monolayers under different subphase conditions. We have used a constant surface pressure insertion assay to assess the degree of peptide insertion into the lipids. Simultaneously, we monitored the surface morphology of the monolayers with fluorescence microscopy. We have also performed dual-probe fluorescence measurements where both the peptide and lipid are tagged with chromophores. Isotherm measurements show that Aβ inserts into both DPTAP and DPPG monolayers under physiologically relevant conditions. Insertion into DPPC occurs at lipid densities below that found in a bilayer. The level of insertion is inversely proportional to the lipid packing density. Our results indicate that lipids need not be anionic to interact with Aβ. Electrostatic effects involved in Aβ40-lipid interaction are discussed.

INTRODUCTION

Alzheimer's disease (AD) is a progressive neurodegenerative disease pathologically characterized by neurofibrillary tangles and neuritic plaques in the brain. Neurofibrillary tangles are due to hyperphosphorylated tau proteins. Instead of associating with microtubules, tau proteins aggregate into insoluble paired helical filaments when hyperphosphorylated (Kosik et al., 1986). The neuritic plaques are extracellular lesions and consist of deposits of amyloid beta (Aβ) peptide. Aβ is a 40- to 43-amino acid residue amphiphilic polypeptide with a hydrophobic C-terminal and a hydrophilic N-terminal (Hardy, 1997; Selkoe, 1994). During regular cell metabolism, Aβ is cleaved from a transmembrane protein called the amyloid beta precursor protein (Haass and Selkoe, 1998). The nonaggregated form of the peptide seems to be a normal constituent of the cerebrospinal fluid (Seubert et al., 1992). The classic neuritic plaques contain dense fibrillar deposits of both Aβ40 and Aβ42. Amorphous, largely nonfibrillar deposits consisting of solely Aβ42 are precursor lesions that lack damaged neurites (axons and dendrites) (Selkoe, 2000). Aβ42 in several regions of the brain is correlated with the development of AD and its clinical progression (Naslund et al., 2000). The secondary structure of the peptide in the fibrous form is predominantly beta-sheet as demonstrated by circular dichroism (Barrow et al., 1992; Terzi et al., 1995), NMR spectroscopy (Coles et al., 1998), and fiber x-ray diffraction (Malinchik et al., 1998). It has been shown by in vitro cell culture studies that the β-structured aggregates are toxic to neurons (Lorenzo and Yankner, 1994; Pike et al., 1993). Whether Aβ aggregation in the brain is a cause or a result of AD is debated (Hardy, 1997), but evidence seems to support the former (Selkoe, 2000). Recently, however, a paradigm shift is emerging as to the nature of the toxic aggregates. Both in vitro and in vivo studies have revealed that soluble, oligomeric forms of Aβ also have potent neurotoxic activities. In fact, these may be the proximate effectors of the neuronal injury and death occurring in AD, and the disease may be caused not by the mature aggregates but by the oligomeric intermediates during the aggregation process itself (Bucciantini et al., 2002; Kirkitadze et al., 2002). Based on these findings, it has even been suggested that Aβ can be ''detoxified'' by converting the oligomeric form to the fibrillar form (Lashuel et al., 2002).

Whether the toxic species are mature aggregates or protofibrils/soluble oligomers, the formation of such entities requires concentrations of up to millimoles of Aβ for short periods, whereas the in vivo deposition of Aβ evolves over long periods of time by the production of nanomolar concentrations in the brain. It has been demonstrated that the presence of lipids can induce the aggregation of Aβ at μM concentrations in similarly short timescales (McLaurin and Chakrabartty, 1997; Terzi et al., 1997). There have been suggestions that toxicity of Aβ may be due to its interaction with cell membranes, whereby ion channels are formed, disrupting the ion equilibria of the cell (Arispe et al., 1993; Hirakura et al., 1999; Kawahara et al., 1997; Lin et al., 1999; Volles and Lansbury, 2003) There is also recent evidence that membrane cholesterol levels may be mediating Aβ fibrillogenesis (Yip et al., 2001), or that lipid peroxidation may play a role in the pathogenesis of AD (Koppaka and Axelsen, 2000). Although the exact extent of Aβ-membrane interaction remains unclear, all these point to the possible role

Submitted March 25, 2004, and accepted for publication May 28, 2004.

Address reprint requests to Ka Yee C. Lee, PhD, Dept. of Chemistry, The University of Chicago, 5735 S. Ellis Ave., Chicago, IL 60637. Tel: 773-702-7068; Fax: 773-702-0805; E-mail: kayeelee@uchicago.edu.

0006-3495/04/09/1732/09 $2.00

doi: 10.1529/biophysj.104.043265

of membrane lipids in Aβ oligomerization and aggregation. There is a general agreement in the literature that electrostatics plays a role and that Aβ interacts with negatively charged lipids (Bokvist et al., 2004; Chauhan et al., 2000; McLaurin and Chakrabartty, 1997; Terzi et al., 1994; Vargas et al., 2000). However, the issue of whether the peptide inserts into membranes remains unsettled. An understanding of the interaction between peptide monomers and lipids is important in elucidating the mechanism of peptide aggregation/lipid peroxidation/ion channel formation.

In this article, we address the role of electrostatics on Aβ insertion into model membranes. The hydrophobic C-terminus of the peptide corresponds to a portion of the transmembrane region of the amyloid beta precursor protein. Since this portion of the peptide is located within the cell membrane before cleavage, it is plausible that the cleaved peptide inserts itself back into the membrane, thus anchoring itself at the membrane surface. The amphipathic nature of the peptide may also lead to higher local peptide concentrations near the membrane surface. The proposition that the amyloid peptide is seeded within the cell membrane and that subsequent oligomerization/fibrillation takes place at the membrane surface reduces the peptides' search for each other in three dimensions to a two-dimensional problem.

Using Langmuir monolayers as model systems, we have examined the interactions between Aβ40 monomers and various lipids as a function of surface pressures and subphase conditions. In addition to isotherm measurements, the surface morphology of the lipid monolayers was monitored with fluorescence microscopy (FM). In particular, we have tested whether anionic lipids are necessary for forming lipid/peptide complexes. Our results indicate that under physiologically relevant conditions, Aβ inserts into electrically charged lipid films. Even at high surface pressures where the monolayer is tightly packed and no apparent insertion is detected, we observe changes in the surface morphology of the lipid films. Our results can be explained by electrostatic arguments.

EXPERIMENTAL PROCEDURES

Materials

The lipids 1,2-dipalmitoylphosphatidylcholine (DPPC), 1,2-dipalmitoylphosphatidylglycerol (DPPG), and 1,2-dipalmitoyl 3-trimethylammonium propane (DPTAP), the fatty acid-labeled fluorescent dyes N-7-Nitrobenz-2-oxa-1, 3-diazol-4-yl-phosphatidylcholine (NBD-PC) and N-7- Nitrobenz-2-oxa-1, 3-diazol-4-yl-phosphatidylglycerol (NBD-PG) were obtained from Avanti Polar Lipids (Alabaster, AL) in powder form, and used without further purification. The headgroup-labeled fluorescent dye Texas Red 1,2-dihexadecanoyl 3-phosphoethanolamine (TR-DHPE) was purchased from Molecular Probes (Eugene, OR). DPPC, DPTAP, NBD-PC, NBD-PG, and TR-DHPE were dissolved in chloroform (high-performance liquid chromatography grade, Fisher Scientific); DPPG was dissolved in chloroform with 10% by volume methanol. All lipid stock solutions had a concentration between 2 and 10 mg/ml. Spreading solutions were prepared by diluting the stock solutions and adding 0.5 mol % of TR-DHPE. The concentrations of the spreading solutions were between 0.2 and 0.5 mg/ml. Monolayer films were spread using a microsyringe (Hamilton, Reno, NV). All lipid solutions were stored at −20°C in glass vials.

Aβ40 was purchased from Anaspec (San Jose, CA) and used without further purification. The molecular mass of the peptide is 4 kD, and it has the amino acid sequence DAEFRHDSGYEVHHQKLVFFAEDVGSNKGAIIGLMVGGVV. Purity was reported to be >95% by high-performance liquid chromatography. The expected molecular weight was confirmed by matrix assisted laser desorption/ionization mass spectrometry. Aβ40 was stored at −20°C in lyophilized form. To insure that the peptide was in monomeric form, it was dissolved in dimethyl sulfoxide (DMSO) at least 2 h before all injection experiments, as this treatment has been reported to deaggregate any existing multimers and render the peptide monomeric (Shen and Murphy, 1995). The concentration of peptide in DMSO was 5 mg/ml. Hexa-fluoro isopropanol, tri-fluoro acetic acid, or tri-fluoro ethanol have also been reported to ensure a monomeric peptide; however, DMSO is the only solvent that does not have surface activity. We found that dissolving the peptide in DMSO is necessary in getting reproducible results.

For dual-probe fluorescence experiments, Aβ40 with cysteine substituted at position 7 was synthesized and then labeled with fluorescein (Choo-Smith et al., 1997). The tagged peptide was a generous gift from Professor Charles Glabe of the University of California at Irvine. Five percent fluorescently labeled peptide was mixed into a peptide solution dissolved in water, and this mixture was injected into the subphase. All subphases were prepared using water from a Milli-Q system (Millipore, Bedford, MA). Phosphate-buffered saline (PBS) subphase at pH 7.4 was prepared with 120 mM NaCl.

Methods

Our experimental setup consists of a custom-made Langmuir trough milled from a solid piece of virgin Teflon (27.5 × 6.25 × 0.63 cm) epoxied to a thin copper plate. The working surface area of the trough is 145 cm^2. The working subphase volume is between 80 ml and 130 ml. Two Teflon barriers are used for symmetric compression with a linear speed of 0.1 mm/s. This speed corresponds to a typical rate of area change of 10^{-2} $Å^2$/molecule·s. Movement of the barriers is achieved by two high-precision translational stages (UTM100, Newport, Irvine, CA) with a resolution of 1.0 μm; this translates to a resolution of $\sim 10^{-4}$ $Å^2$/molecule for a typical experiment. Compression ratio for the trough from being fully expanded to fully compressed is 7. Temperature control of the subphase is accomplished using six thermoelectric cooling elements connected in series (Marlow Industries, Dallas, TX). These thermoelectric cooling elements are sandwiched between two copper plates, one to which the trough is mounted and the other connected to a constant-temperature water bath (Neslab Instruments, Portsmouth, NH). The subphase temperature is monitored by a submerged Teflon-coated thermistor (Omega Technologies, Stamford, CT). The trough can be operated in a temperature range of 5–45°C. A piece of thin glass coated with indium tin oxide (Delta Technologies, Dallas, TX), which can be resistively heated, is placed over the trough to suppress evaporation and prevent condensation on the microscope objective. The temperature of the glass is monitored by a thermistor (Omega Technologies) and is typically maintained slightly above the subphase temperature to minimize convective currents above the monolayer. A stationary Wilhelmy balance located at the center of the trough (Riegler and Kirstein, Berlin, Germany) is used to measure the surface pressure through a hole in the cover-glass.

Fluorescence microscopy

To monitor the surface morphology of the monolayer, a Nikon optical microscope is positioned above the trough. A 20× or a 50× extra-long working distance objective can be attached to the microscope. The trough is mounted on motorized *xyz* translational stages (Newport, Irvine, CA). The *z* axis is for focusing and the *x* and *y* axes are for translating the trough to

observe different regions of the monolayer. A 100-W high-pressure mercury lamp is used for fluorescence excitation. A dichroic mirror/filter cube is used to direct light onto the monolayer and to filter the emitted fluorescence. Fluorescence is collected by a silicon intensified target camera (Hamamatsu, Bridgewater, NJ). The whole trough/microscope assembly is mounted on a vibrationally isolated table from Newport. The setup is controlled by a custom-made graphical interface using LabView (National Instruments, Austin, TX). Images are recorded with a JVC Super VHS VCR (JVC Co. of America, Wayne, NJ) and digitized using software from ATI technologies. Image analysis is performed using Adobe Photoshop software.

Constant pressure assay

Insertion studies using Langmuir monolayers is a sensitive tool for studying lipid-protein and lipid-peptide interactions (Hanakam et al., 1996). The method can be employed by keeping the surface area or the surface pressure constant. We have monitored the interaction of Aβ40 with lipids using a constant surface pressure assay. Surface pressure is defined as the difference in surface tension between a pure air-fluid interface and one with a monolayer adsorbed. We have used a lipid monolayer to mimic the outer leaflet of a membrane bilayer. Constant-pressure assays were performed by spreading a desired lipid onto a subphase free of Aβ40 peptide, and then compressing the lipid film to a predetermined surface pressure. This pressure was chosen to be between 23 and 30 mN/m for relevance to physiological conditions as the lipid-packing density of a bilayer is reported to be roughly equal to that of a monolayer at around 30 mN/m (Seelig, 1987). Once the desired surface pressure was reached, it was kept constant via a feedback loop built into our apparatus. Twenty μl of 5 mg/ml Aβ40 in DMSO was then aliquoted out, topped off with 500 μl water, and immediately injected into a 90-ml subphase. To avoid disturbing the lipid film, an L-shaped syringe (Hamilton, Reno, NV) was used for injecting the peptide from underneath one of the barriers. After peptide injection, the effective relative change in area per lipid molecule ($\Delta A/A$) was monitored. In this constant-pressure mode, insertion of the peptide into the lipid leads to an increase in the lipid surface area. Conversely, the surface area would decrease if the peptide causes the lipid monolayer to dissolve in the subphase. In all experiments, the average concentration of the peptide in the total subphase volume after injection was 250 nM and the temperature of the subphase was 30°C. This concentration was well below the critical micelle concentration of Aβ40, which was reported to be around 12.5 μM (Pike et al., 1993). It should be noted that if the surface area, instead of the surface pressure, were held constant, peptide insertion into the lipid film would result in an increase in surface pressure.

Three lipids were examined to investigate the effect of headgroup charge on their ability to interact with Aβ peptides: zwitterionic DPPC, anionic DPPG, and cationic DPTAP. Although saturated lipids are not in abundance in the cell membrane, these lipids were chosen in our study because they exhibit a two-phase coexistence region at the temperature and surface pressures examined, enabling us to perform FM simultaneously with the isotherm measurements. Half a mole percent TR-DHPE was incorporated into the spreading solution. The dye molecules are covalently bonded to the hydrophilic lipid headgroup region. Due to steric reasons, the dye partitions into the fluid phase, rendering it bright and the condensed phase dark (Knobler, 1990). To ensure that our results are not artifacts due to the bulky TR-labeled DHPE molecules interacting with Aβ40, we have repeated fluorescence experiments by replacing TR-DHPE with 1% by mole fluorescent NBD-PC for DPPC, and 1% by mole NBD-PG for DPPG. The NBD moiety is covalently attached to the hydrocarbon tails of the lipids, thereby diminishing its accessibility to the Aβ40 peptide. As TR-DHPE has a higher quantum yield than NBD, it is necessary to double the mole percentage from ½ to 1 when switching from TR to NBD to achieve similar contrast in the micrographs. To ensure that the changes observed with FM are due to interactions with the peptide and not an artifact of the injection protocol, we have performed control experiments where blank solution is injected into the subphase, and it does not alter lipid morphology.

RESULTS

We first examined the subphase dependence of the surface activity of Aβ40 and found that the activity of the peptide increased with increasing ionic strength. Upon injection into pure water at 30°C, Aβ40 achieved an equilibrium surface pressure of 12 mN/m. In PBS subphase, the surface pressure was 15 mN/m. Increasing saline concentration of the buffered subphase from 120 mM to 240 mM increased Aβ40 surface activity further, resulting in a surface pressure of 17 mN/m (Fig. 1). The timescale for Aβ40 surface adsorption is also dependent on the subphase conditions. Surface pressure profile upon Aβ40 injection changes from a sigmoidal rise in water subphase to an asymptotically increasing one in PBS.

We have carried out constant-pressure measurements with DPPG, DPPC, and DPTAP monolayers under different surface pressure and subphase conditions. The total relative change in area ($\Delta A/A$), obtained after reaching a steady-state plateau (typically between 1.5 and 5 h after Aβ40 injection) are summarized in Table 1 as a function of surface pressure, lipid identity, and subphase conditions. Although cationic lipids are not found under physiological conditions, zwitterionic DPPC, anionic DPPG, and cationic DPTAP were chosen to provide a full spectrum in examining the role of headgroup electrostatics on the interaction of Aβ40 with lipids. Table 1 clearly indicates that Aβ40 inserts much more readily into DPPG and DPTAP monolayers than DPPC under similar conditions in both pure water and PBS subphase.

For a typical constant-pressure experiment, the lipid monolayer was spread at the interface with a high surface area per molecule to ensure the film remains at gas-liquid phase coexistence, thus guaranteeing the formation of a homogeneous film. Compression of the film did not occur until at least 5 min after the initial spread to allow for solvent

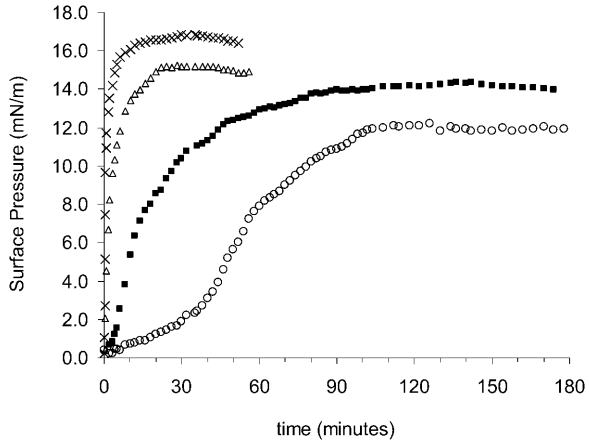

FIGURE 1 Change in surface pressure as a function of time upon injection of Aβ40 into different subphases: (○) water, (■) pH=7.4 phosphate buffer, (△) phosphate buffer with 120 mM NaCl, and (×) phosphate buffer with 240 mM NaCl. The time of injection is taken as $t = 0$. The concentration of Aβ in the subphase is 250 nM, and the subphase temperature is 30°C.

TABLE 1 Percentage change in lipid area upon Aβ insertion

	Pressure	Pure water		PBS	
DPPC	23 mN/m	4		6	
	25 mN/m	<2	Dipole-dipole	2	Ion-dipole
	30 mN/m	-		-	
DPPG	23 mN/m	140		13	
	25 mN/m	108	Ion-dipole	10	Ion-ion (repulsive)
	30 mN/m	14		<2	
DPTAP	23 mN/m	144		79	
	25 mN/m	89	Ion-dipole	34	Ion-ion (attractive)
	30 mN/m	35		4	

Percentage area change as Aβ peptides insert into lipid monolayers as a function of lipid identity, surface pressure, and two different subphase conditions. The concentration of Aβ in the subphase is 250 nM, and $T = 30°C$ for all experiments. The nature of the electrostatic interaction between the lipid and the peptide is also indicated. The calculated net charge of Aβ is 0 in pure water (pH 5.5), and −3 in PBS (pH 7.4).

evaporation. Fig. 2 *A* shows the pressure area isotherm of a DPPG film spread at ~118 Å^2/molecule on pure water. The DPPG film was compressed to 25 mN/m (indicated by an arrow in Fig. 2 *A*), after which the pressure was held constant. Aβ was then injected into the subphase. The area per DPPG molecule was 45 Å^2 at the time of peptide injection. This point is marked with an arrow in the figure. Subsequent insertion of Aβ40 resulted in an increase in the surface area. Fig. 2 *B* shows the corresponding relative change in area per molecule after peptide injection as a function of time. The moment of peptide injection was taken to be $t = 0$. Within 2 h after injection, the effective area per lipid molecule reached ~92 Å^2. The change is roughly 105%, as shown in Fig. 2 *B*.

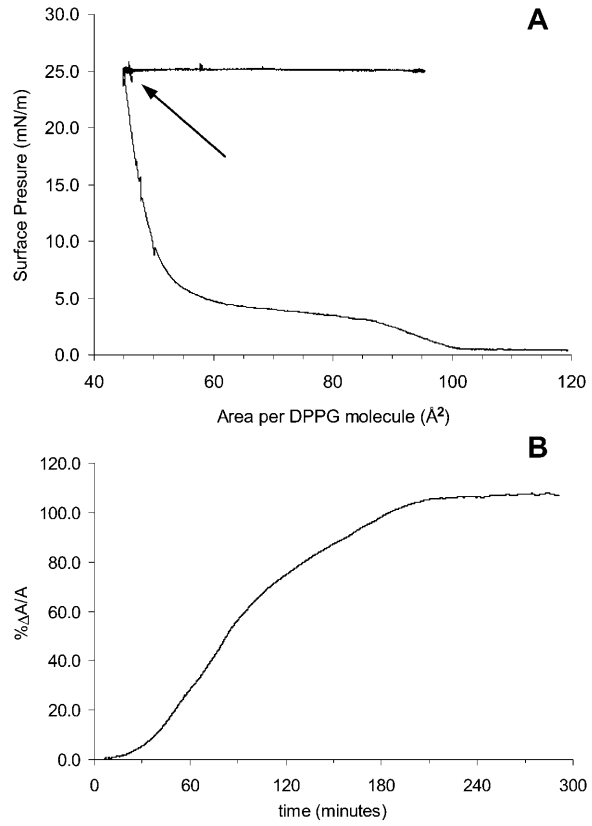

FIGURE 2 (*A*) Isotherm showing the increase in area per DPPG molecule upon Aβ40 injection at a constant surface pressure of 25 mN/m. The arrow marks the time of peptide injection. (*B*) The corresponding percentage change in area per molecule as a function of time upon injection. Time zero corresponds to the moment of peptide injection. Temperature is 30°C and subphase is pure water.

The morphological changes of the DPPG monolayer resulting from Aβ40 injection are shown in Fig. 3. Fig. 3 *A* shows the FM image of the DPPG monolayer at 25 mN/m before the injection of Aβ into the subphase. The ordered condensed phase is dark since the dye is excluded from the ordered domains due to steric hindrance. The less ordered phase, termed liquid-expanded phase, is bright as a result of dye partitioning. As clearly demonstrated by the image (Fig. 3 *A*), most of the DPPG film is in the condensed phase at 25 mN/m under the given experimental conditions. Fifteen min after injection of peptide (Fig. 3 *B*), the ratio of dark to bright regions is reduced. The reduction becomes more pronounced with time (Fig. 3 *C*) as Aβ disrupts lipid packing and decreases the size of the dark ordered condensed domains while increasing that of the disordered phase. The peptide also induces fuzziness at domain boundaries, suggesting that the phase boundaries could be the preferred locations for peptide insertion. At 150 min after injection (Fig. 3 *D*), the boundary between the ordered and disordered regions became less sharp with the emergence of a gray phase. Insertion into DPPG monolayers at 30 mN/m shows similar trends, resulting in both area increase and morphological changes (data not shown), though to a lesser extent (Table 1).

For a DPTAP monolayer at 25 mN/m on pure water, the change in total area is 89% after the injection of Aβ. Fig. 4 *A* shows the corresponding progression in the surface morphol-

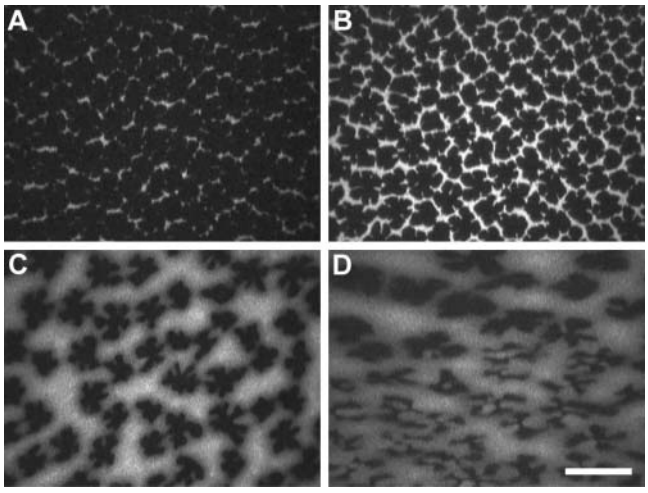

FIGURE 3. Domain morphology of a DPPG monolayer on a water subphase at 30°C and a constant surface pressure of 25 mN/m. Images were taken (*A*) before, (*B*) 15 min after, (*C*) 45 min after, and (*D*) 2.5 h after injection of peptide. The scale bar is 100 μm.

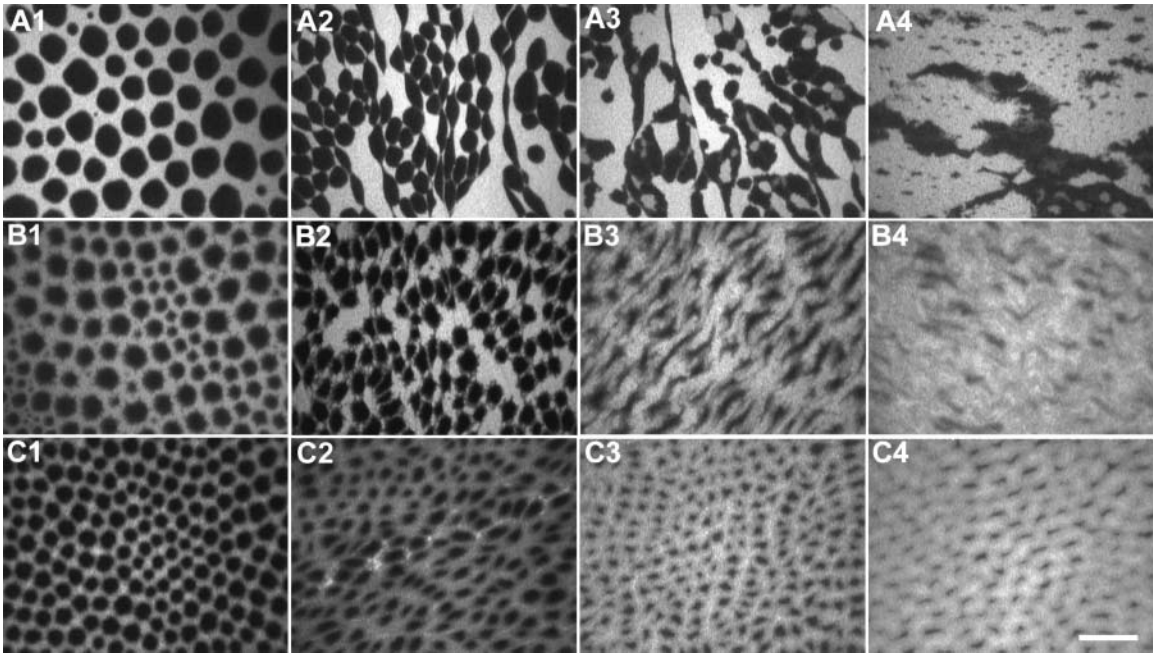

FIGURE 4 Domain morphology of a DPTAP monolayer on a water subphase at a constant surface pressure of (*A*) 25 and (*B*) 30 mN/m, and (*C*) on PBS subphase at 30 mN/m. Images were taken (*1*) before injection, (*2*) right after injection, (*3*) 45–60 min after injection, and (*4*) 2–4 h after injection. For all cases, temperature is 30°C, Aβ40 concentration in the subphase is 250 nM, and the scale bar is 100 μm. The fringes extending from the domains in *B1* are due to an instability of the condensed DPTAP domain shape under the given experimental conditions, and can also be seen for DPPC in Fig. 5 *A1* (Diamant et al., 2001).

ogy of the monolayer. By 4 h after Aβ injection (Fig. 4 *A4*), the surface morphology shows no resemblance to that before peptide injection (Fig. 4 *A1*). The peptide initially causes the dark condensed-phase domains to coalesce (Fig. 4 *A2*) and thereafter significantly reduces the amount of condensed-phase domains. The morphological changes are just as prominent at 30 mN/m, and the decrease in condensed to fluid lipid area fraction is apparent (Fig. 4 *B*). On a PBS at 30 mN/m, the condensed-phase domains are reduced in size (Fig. 4 *C*) but not as drastically as for the same pressure in pure water (Fig. 4 *B*). Even 2 h after peptide injection, residual condensed domains are still discernable (Fig. 4 *C4*).

In the case of DPPC, the amount of insertion is much less compared to DPPG or DPTAP in both water and PBS. Nevertheless, at 23 mN/m in PBS, a 6% area change is accompanied by a visible decrease in the amount of condensed-phase domains (Fig. 5 *A*). Even under conditions where there is no significant change in the area after Aβ40 is injected into the subphase (e.g., at 30 mN/m), we observe significant changes in the shape and distribution of the domains. Fig. 5 *B* shows how the condensed-phase domains of DPPC on a water subphase at a surface pressure of 25 mN/m abandon their discrete domain structure and coalesce upon Aβ injection. In this case, the recorded area change is $<2\%$ (Table 1). Although the amount of increase in insertion going from water to PBS is small, the difference is statistically significant and if the salt concentration is increased to 240 mM NaCl, the amount of insertion at 25 mN/m goes up to 7% (Fig. 6).

To identify the location of the peptide in the lipid matrix, we have carried out dual probe fluorescence measurements. Fluorescein-labeled peptides were used to insert into TR-labeled lipids at a surface pressure of 30 mN/m for DPPG and DPTAP. The images shown are for a pure water subphase for DPPG and PBS subphase for DPTAP (Fig. 7). Fluorescence images were obtained for the two different emission wavelengths by switching the filter cubes to

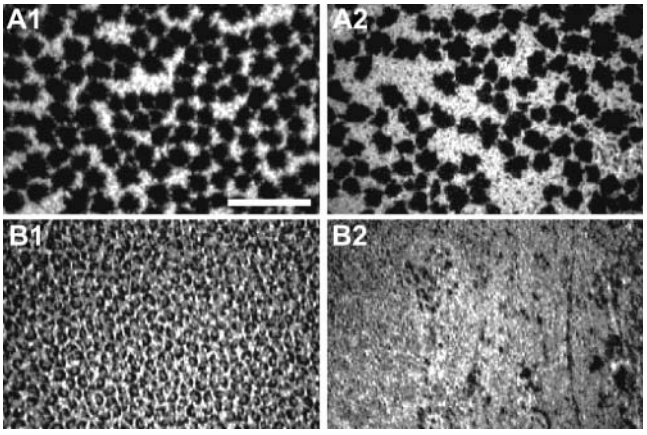

FIGURE 5 Domain morphology of a DPPC monolayer (*A*) on a PBS subphase at a constant surface pressure of 23 mN/m; and (*B*) on a pure water subphase at 25 mN/m. Images were taken (*1*) before and (*2*) 10 min or 2 h after injection for the PBS (*A2*) and water (*B2*) subphases, respectively. The scale bar is 100 μm.

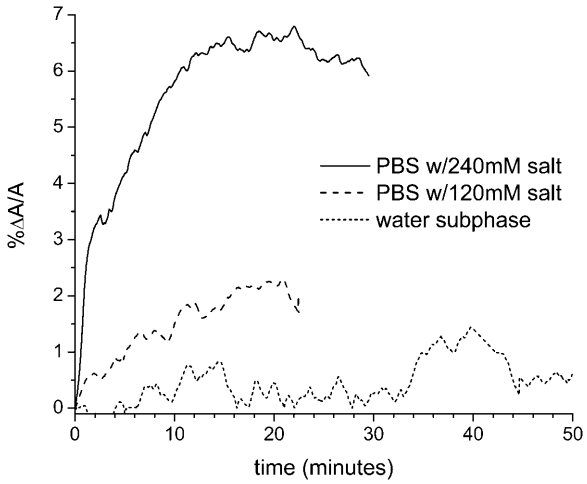

FIGURE 6 The percentage change in area per DPPC molecule as a function of subphase conditions upon injection of Aβ40 at a constant surface pressure of 25 mN/m. Time zero corresponds to the moment of peptide injection. Subphase temperature is 30°C.

correlate the location of the peptide with the phase of the lipid monolayer. For DPPG monolayers, the peptide inserts preferentially into the disordered region of the film, as indicated by the correspondence between the bright and gray phases in the fluorescence micrograph showing the tagged lipid (Fig. 7 *A*) and the bright phase in that for the tagged peptide (Fig.7 *B*). Preference for the disordered region of the monolayer is also found for DPPC on PBS subphase (data not shown). In the case of DPTAP, however, fluorescence from the peptide is uniform in the monolayer, and no preference for the disordered region is found (Fig. 7, *C* and *D*).

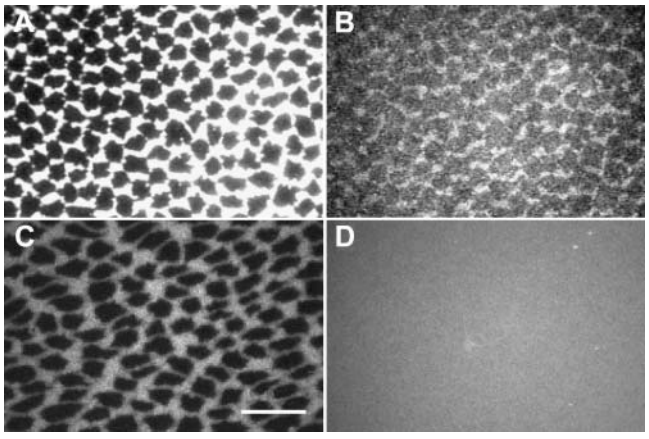

FIGURE 7 Dual probe fluorescence micrographs of (*A* and *B*) DPPG and (*C* and *D*) DPTAP show the different modes of interaction with Aβ40. Left panels show fluorescence from the emission of Texas-Red dye tagged to the lipid; right panels show that of fluorescein tagged to Aβ40. The DPPG film was at 30 mN/m on a pure water subphase and the DPTAP film was at 30 mN/m on PBS. Both experiments were performed at 30°C. The scale bar is 100 μm.

DISCUSSION

To understand the role of membrane lipids in mediating the behavior of Aβ peptides, we have examined the interaction between model lipid membranes and monomeric Aβ peptides. Our membrane model is an approximation to the outer leaflet of the cell membrane. Although cationic lipids are not present in human cell membrane, using DPTAP is critical to understand the role of charge on peptide adsorption. The interaction between Aβ and phospholipids has been investigated previously with mixed conclusions regarding the insertion of the peptide into membranes. Results from vesicle rupture/dye release experiments (McLaurin and Chakrabartty, 1997) support insertion under physiological conditions whereas monolayer experiments (Terzi et al., 1997) demonstrate otherwise. Other results suggest there may be two different modes of interaction where the peptide may be adsorbed onto or inserted into membranes (Bokvist et al., 2004). There is, nonetheless, a general agreement that Aβ prefers to bind to negatively charged or acidic phospholipids. Alternatively, our results demonstrate that cationic lipids can interact with Aβ just as strongly as anionic lipids, which are in agreement with a recent report by Kremer et al. (2001).

Constant-pressure assays show that the level of change in the effective area occupied by a phospholipid molecule after the introduction of Aβ peptides into the subphase is a function of subphase conditions, as well as pressure and identity of the lipid monolayer employed. In the pure water case, we have observed a significantly higher level of insertion for the peptide into the charged lipid monolayers of DPTAP and DPPG as opposed to the zwitterionic DPPC films. This can be understood in terms of the ion-dipole interaction between the lipid and the peptide in the former case and the weaker dipole-dipole interaction in the latter case when the subphase used is pure water (Table 1).

In PBS, the level of insertion of the peptide into charged lipid monolayers is still higher than that observed in zwitterionic films, with the greatest insertion observed with DPTAP. When the subphase condition changes from pH 5.5 (pure water) to pH 7.4 (PBS), the three histidine residues turn from positively charged to neutral by losing a proton, leaving the peptide with a net negative charge (although surface pH may be slightly lower than bulk pH, the effect is not large enough to lower the pH to the isoelectric point of the peptide (Bostrom et al., 2002)). It is therefore logical for the peptide to interact more favorably with the positively charged DPTAP monolayers compared to the zwitterionic DPPC or anionic DPPG monolayers. It should be noted that there is still substantial insertion of the negative peptide into anionic DPPG monolayers, despite the fact that both have similar charges. This can be accounted for by the fact that whereas the peptide has an overall negative charge, there remain positively charged residues that can interact favorably with the anionic DPPG molecules. Nonetheless, the overall negative charge on the peptide substantially reduces the level of insertion into

DPPG as compared to DPTAP under buffered saline conditions.

In comparing the effect of subphase conditions, we note that the propensity of the peptide to adsorb to the air-water interface increases in PBS compared to pure water (Fig. 1). In water the peptide monomers can be approximated as dipoles, and these dipoles have a characteristic packing at the air-water interface. In PBS the peptide has an overall charge of −3. The interaction between the charged peptides in the presence of screening salt becomes equivalent to the one between dipoles because of the oppositely charged cloud of counter ions. Thus, as the subphase salt concentration is increased with subsequent decrease in the screening length, one may be able to reach a regime where the effective dipole moments are weaker than the real dipole of the peptide in pure water (Andelman et al., 1987). One therefore expects that with everything else held constant, the amount of insertion should increase going from pure water to PBS. However, this effect is observed only in the case of DPPC. For DPPG, the effect is offset by the electrostatic repulsion with the peptide, as explained above. What is puzzling is the case for DPTAP. Aβ40 inserts much more readily into DPTAP in pure water than in buffered saline. As mentioned earlier, the peptide is neutral in pure water but carries an overall negative charge in buffered saline. With both pH and ionic strength effects pointing to an increase in insertion in PBS, why then would a peptide insert less into a cationic lipid film when it is in an anionic state as opposed to a zwitterionic state? The answer, we propose, lies in the strong electrostatic interaction between the cationic lipid headgroup and the anionic peptide. This interaction is so dominant that the peptide is strongly attracted and trapped in the headgroup area instead.

To check this hypothesis, we have carried out dual-probe experiments in which fluorescein-labeled peptides were used to insert into TR-labeled lipids. These experiments clearly indicate that in PBS subphase, Aβ40 does not differentiate between condensed versus fluid regions but adsorbs uniformly onto the DPTAP film. This result is consistent with our hypothesis that the attractive electrostatic interaction between DPTAP and Aβ40 overwhelms the additional gain in energy resulting from the insertion of Aβ40 into the lipid film. To further substantiate our hypothesis and obtain a quantitative picture of where and how Aβ lies on the membrane surface, we are studying the effect of Aβ40 on DPPC, DPPG, and DPTAP using grazing-incidence x-ray diffraction, x-ray reflectivity, and neutron reflectivity.

For all surface pressures where there is insertion we detect via FM that Aβ disrupts the ordered phase of the lipids. This is true even under conditions where we see minimal (Fig. 5 *B*) or no insertion (data not shown), indicating that Aβ causes surface reorganization of the lipids. We observe that when there is insertion, the boundary between the ordered and disordered regions becomes fuzzy, suggesting that the phase boundaries could be the preferred locations for the peptide. However, this does not imply that a two-phase coexistence of the lipids is necessary for peptide insertion. In fact, we have observed insertion of the peptide into single-phase films formed by unsaturated phospholipids under similar experimental conditions (data not shown).

It should be pointed out again that the electrostatic effects on peptide insertion have two contributing factors: the overall change in peptide charge due to pH adjustments, and the alterations in screening length due to changes in ionic strength. In this article, comparisons are drawn between peptide insertion into lipid films on a pure water subphase and that with a buffered saline subphase, whereby both the pH and the ionic strength are altered simultaneously. Although it is difficult to decouple the effects of pH from those of ionic strength with only the data presented here, one should be able to do so if one parameter is changed at a time. This should also enable one to determine which factor is dominant. Indeed we have performed another set of insertion experiments at pH 7.4 phosphate buffer with no additional salt (data not shown). Under this subphase condition, we have observed a slight increase in insertion in DPPC but a decrease in both DPPG and DPTAP when compared to results at pH 5.5. Such changes in the insertion profiles for all three lipids are qualitatively similar to those observed at pH 7.4 with 120 mM NaCl. Hence, changes in the overall peptide charge brought about by adjusting the pH play a more dominant role than changes due to the ionic strength in determining the level of peptide insertion. The addition of 120 mM NaCl to the pH 7.4 subphase merely results in an increase in the level of insertion for all three lipids. In fact, the increase in insertion for both DPPG and DPTAP is small enough to be offset by the decrease resulting from peptide charge effects due to pH change, whereas for DPPC, both effects are in the same direction, resulting in an overall increase in insertion. These observations suggest that an increase in the ionic strength of the subphase leads to a corresponding increase in the peptide's propensity to associate with the interface. We have carried out experiments at an even higher salt concentration of 240 mM NaCl and have observed that this trend continues to persist. For pure peptide adsorption, we have shown in Fig. 1 that the surface activity of the peptide increases with ionic strength. For peptide insertion into a lipid film, Fig. 6 demonstrates that the level of insertion is further enhanced when the ionic strength is changed from 120 mM to 240 mM. Since both sets of experiments were performed at constant pH, the observed changes can only be attributed to the increased ionic strength, which seems to produce an enhanced hydrophobic effect.

Although electrostatics is likely to play a major role in determining the level of insertion, there can be other factors that contribute to the phenomena observed. One plausible factor is the head-tail mismatch of the lipids. The tail groups of the three lipids studied are identical, but the headgroups are different. DPPC has a larger headgroup than both DPPG and DPTAP. DPPG molecules are able to tightly pack with the tails arranged in a hexagonal fashion at high surface pressure; DPTAP, and to a greater extent DPPC, cannot pack as tightly

due to a head-tail mismatch, causing their tailgroups to be tilted even at high surface pressures (Ege, 2004). On this basis alone, one would expect insertion to favor DPPC over DPTAP and DPPG in the given order. Our measurements, however, indicate otherwise, leading us to conclude that the head-tail mismatch is not a significant factor in determining peptide insertion. Experiments are currently underway to explore the effect of unsaturation in the tailgroup on peptide insertion.

In a recent article, Bokvist et al. (2004) discuss a model where Aβ40 interacts with mixed DMPC/DMPG vesicles (where DMPC and DMPG have headgroups identical to DPPC and DPPG, respectively, but have hydrocarbon tails that are 14 carbons long instead of 16). They differentiate between two modes of interaction: where the peptide, when added into a vesicle solution, is adsorbed on the surface of the vesicles and causes aggregation; or where, when the vesicles are prepared with peptide present, the peptide is inserted and bound to the vesicles and is stable so that no aggregation occurs. Our experimental results for DPPG in PBS show that Aβ40 does not insert to an appreciable extent into DPPG at packing densities relevant to that found in vesicles. Though the insertion assay used cannot detect if Aβ40 is adsorbed underneath the monolayer, FM shows that DPPG morphology changes even though insertion is minor (a similar morphological change of DPPC at conditions of low peptide insertion is seen in Fig. 5 *B*). The change in morphology of the monolayer suggests that the peptide is associated with the lipid surface, consistent with the findings of Bokvist et al. (2004).

The electrostatic explanation we propose does not consider the detailed structure of the peptide but treats it as a large ion (or a dipole in the case of water subphase). The argument given thus accounts for the ability of the peptide to find the membrane surface. Insertion into the membrane, however, is motivated by the stabilization of the hydrophobic tail of Aβ40. For this reason, the longer version of the peptide, Aβ42, with the additional residues isoleucine and alanine, can be predicted to insert into membranes to a greater extent. The extent of insertion can be quantified by x-ray reflectivity measurements that are currently underway. The additional hydrophobic residues also make Aβ42 more prone to aggregation.

Finally, we would like to briefly discuss the issue of oligomerization and how it may contribute to the observed differences in peptide insertion. The oligomeric form of the peptide has been receiving increased attention as the speculated culprit of AD. We have preliminary evidence suggesting that the oligomeric form of the peptide (obtained by aging peptide monomers in water) inserts to a greater extent into lipid films compared to its monomeric counterpart. Although the insertion results in Table 1 do not contain information on the kinetics of insertion, some of the figures presented show the time course of surface adsorption of the peptide (Fig. 1) and peptide insertion into lipid films (Figs. 2 *B* and 6). These figures capture the differences in insertion kinetics for water subphase versus PBS. It is obvious from Fig. 1 that the lag time for surface association found in water is greatly reduced and eventually eliminated with increased ionic strength. As already discussed, increases in ionic strength seem to enhance the hydrophobicity of the peptide, which can be stabilized by peptide insertion into the lipid film and/or lipid oligomerization. Since both mechanisms would result in accelerated surface association, both could contribute to the observed decrease in lag time.

Since the formation of soluble, toxic oligomers has been proposed to be a key pathogenic process in AD (Bucciantini et al., 2002), an understanding of the interaction of Aβ with membranes becomes more valuable as it pertains to the toxicity mechanism. It is clear that under conditions where Aβ40 can insert into membranes extensively, the alteration to the membrane is considerable, possibly to the extent of affecting its proper functioning. A relevant issue that arises from our work is to distinguish between monomeric species versus oligomeric species inserting into the membrane. Two possibilities are that peptide inserts as a monomer and transposes its environment to initiate aggregation into oligomers/protofibrils or that the peptide oligomerizes and then inserts into membranes to stabilize itself. Studies are underway to examine these two possible scenarios.

A clear trend from our results is the decrease in insertion with corresponding increase in surface pressure for all three lipids. This is not surprising: at high surface pressures where the hydrocarbon chains of the lipids are tightly packed, the peptide cannot insert easily. However, one can envision that the peptide can readily insert into damaged cells where the membrane integrity is compromised, or if negatively charged lipids of the inner leaflet of the cell membrane are somehow exposed to the extracellular region. In this context, it is worthwhile to take into account the effect of aging or damage (e.g., oxidative damage) on cell membrane function when discussing AD.

We are indebted to Prof. Charles Glabe for first pointing out to us the problem of Aβ-lipid interaction and for many stimulating discussions. We are grateful also for his generous gift of the tagged peptide used in the experiments presented here and for providing us with Aβ40 and Aβ42 when we started this project. We thank Prof. Haim Diamant for helpful discussions.

This work was funded by the Alzheimer's Association (IIRG-9901175) and the American Health Assistance Foundation (A1999057). The experimental apparatus was made possible by a National Science Foundation Chemistry Research Instrumentation and Facilities Program/Junior Faculty grant (CHE-9816513). C.E. was partially supported by the National Science Foundation Materials Research and Engineering Centers Program under DMR-0213745.

REFERENCES

Andelman, D., F. Brochard, and J. F. Joanny. 1987. Phase-transitions in Langmuir monolayers of polar-molecules. *J. Chem. Phys.* 86:3673–3681.

Arispe, N., E. Rojas, and H. B. Pollard. 1993. Alzheimer disease amyloid beta protein forms calcium channels in bilayer membranes: blockade by tromethamine and aluminum. *Proc. Natl. Acad. Sci. USA.* 90:567–571.

Barrow, C. J., A. Yasuda, P. T. Kenny, and M. G. Zagorski. 1992. Solution conformations and aggregational properties of synthetic amyloid beta-peptides of Alzheimer's disease. Analysis of circular dichroism spectra. *J. Mol. Biol.* 225:1075–1093.

Bokvist, M., F. Lindstrom, A. Watts, and G. Grobner. 2004. Two types of Alzheimer's beta-amyloid (1–40) peptide membrane interactions: aggregation preventing transmembrane anchoring versus accelerated surface fibril formation. *J. Mol. Biol.* 335:1039–1049.

Bostrom, M., D. R. M. Williams, and B. W. Ninham. 2002. Influence of Hofmeister effects on surface pH and binding of peptides to membranes. *Langmuir.* 18:8609–8615.

Bucciantini, M., E. Giannoni, F. Chiti, F. Baroni, L. Formigli, J. Zurdo, N. Taddei, G. Ramponi, C. M. Dobson, and M. Stefani. 2002. Inherent toxicity of aggregates implies a common mechanism for protein misfolding diseases. *Nature.* 416:507–511.

Chauhan, A., I. Ray, and V. P. Chauhan. 2000. Interaction of amyloid beta-protein with anionic phospholipids: possible involvement of Lys28 and C-terminus aliphatic amino acids. *Neurochem. Res.* 25:423–429.

Choo-Smith, L. P., W. Garzon-Rodriguez, C. G. Glabe, and W. K. Surewicz. 1997. Acceleration of amyloid fibril formation by specific binding of Abeta-(1–40) peptide to ganglioside-containing membrane vesicles. *J. Biol. Chem.* 272:22987–22990.

Coles, M., W. Bicknell, A. A. Watson, D. P. Fairlie, and D. J. Craik. 1998. Solution structure of amyloid beta-peptide(1–40) in a water-micelle environment. Is the membrane-spanning domain where we think it is? *Biochemistry.* 37:11064–11077.

Diamant, H., T. A. Witten, C. Ege, A. Gopal, and K. Y. Lee. 2001. Topography and instability of monolayers near domain boundaries. *Phys Rev E.* 63:061602–061612.

Ege, C. 2004. Interaction of amyloid beta peptides with lipid membranes. PhD Thesis. The University of Chicago, Chicago.

Haass, C., and D. J. Selkoe. 1998. Alzheimer's disease. A technical KO of amyloid-beta peptide. *Nature.* 391:339–340.

Hanakam, F., G. Gerisch, S. Lotz, T. Alt, and A. Seelig. 1996. Binding of hisactophilin I and II to lipid membranes is controlled by a pH-dependent myristoyl-histidine switch. *Biochemistry.* 35:11036–11044.

Hardy, J. 1997. Amyloid, the presenilins and Alzheimer's disease. *Trends Neurosci.* 20:154–159.

Hirakura, Y., M. C. Lin, and B. L. Kagan. 1999. Alzheimer amyloid abeta1–42 channels: effects of solvent, pH, and Congo Red. *J. Neurosci. Res.* 57:458–466.

Kawahara, M., N. Arispe, Y. Kuroda, and E. Rojas. 1997. Alzheimer's disease amyloid beta-protein forms Zn(2+)-sensitive, cation-selective channels across excised membrane patches from hypothalamic neurons. *Biophys. J.* 73:67–75.

Kirkitadze, M. D., G. Bitan, and D. B. Teplow. 2002. Paradigm shifts in Alzheimer's disease and other neurodegenerative disorders: the emerging role of oligomeric assemblies. *J. Neurosci. Res.* 69:567–577.

Knobler, C. M. 1990. Seeing phenomena in flatland–studies of monolayers by fluorescence microscopy. *Science.* 249:870–874.

Koppaka, V., and P. H. Axelsen. 2000. Accelerated accumulation of amyloid beta proteins on oxidatively damaged lipid membranes. *Biochemistry.* 39:10011–10016.

Kosik, K. S., C. L. Joachim, and D. J. Selkoe. 1986. Microtubule-associated protein tau (tau) is a major antigenic component of paired helical filaments in Alzheimer disease. *Proc. Natl. Acad. Sci. USA.* 83: 4044–4048.

Kremer, J. J., D. J. Sklansky, and R. M. Murphy. 2001. Profile of changes in lipid bilayer structure caused by beta-amyloid peptide. *Biochemistry.* 40:8563–8571.

Lashuel, H. A., D. Hartley, B. M. Petre, T. Walz, and P. T. Lansbury, Jr. 2002. Neurodegenerative disease: amyloid pores from pathogenic mutations. *Nature.* 418:291–292.

Lin, H., Y. J. Zhu, and R. Lal. 1999. Amyloid beta protein (1–40) forms calcium-permeable, Zn2+-sensitive channel in reconstituted lipid vesicles. *Biochemistry.* 38:11189–11196.

Lorenzo, A., and B. A. Yankner. 1994. Beta-amyloid neurotoxicity requires fibril formation and is inhibited by congo red. *Proc. Natl. Acad. Sci. USA.* 91:12243–12247.

Malinchik, S. B., H. Inouye, K. E. Szumowski, and D. A. Kirschner. 1998. Structural analysis of Alzheimer's beta(1–40) amyloid: protofilament assembly of tubular fibrils. *Biophys. J.* 74:537–545.

McLaurin, J., and A. Chakrabartty. 1997. Characterization of the interactions of Alzheimer beta-amyloid peptides with phospholipid membranes. *Eur. J. Biochem.* 245:355–363.

Naslund, J., V. Haroutunian, R. Mohs, K. L. Davis, P. Davies, P. Greengard, and J. D. Buxbaum. 2000. Correlation between elevated levels of amyloid beta-peptide in the brain and cognitive decline. *JAMA.* 283:1571–1577.

Pike, C. J., D. Burdick, A. J. Walencewicz, C. G. Glabe, and C. W. Cotman. 1993. Neurodegeneration induced by beta-amyloid peptides in vitro: the role of peptide assembly state. *J. Neurosci.* 13:1676–1687.

Seelig, A. 1987. Local anesthetics and pressure: a comparison of dibucaine binding to lipid monolayers and bilayers. *Biochim. Biophys. Acta.* 899: 196–204.

Selkoe, D. J. 1994. Cell biology of the amyloid beta-protein precursor and the mechanism of Alzheimer's disease. *Annu. Rev. Cell Biol.* 10: 373–403.

Selkoe, D. J. 2000. Toward a comprehensive theory for Alzheimer's disease. Hypothesis: Alzheimer's disease is caused by the cerebral accumulation and cytotoxicity of amyloid beta-protein. *Ann. N. Y. Acad. Sci.* 924:17–25.

Seubert, P., C. Vigo-Pelfrey, F. Esch, M. Lee, H. Dovey, D. Davis, S. Sinha, M. Schlossmacher, J. Whaley, C. Swindlehurst, R. McCormak, R. Wolfbert, D. Selkoe, I. Lieberburg, and D. Schenk. 1992. Isolation and quantification of soluble Alzheimer's beta-peptide from biological fluids. *Nature.* 359:325–327.

Shen, C. L., and R. M. Murphy. 1995. Solvent effects on self-assembly of beta-amyloid peptide. *Biophys. J.* 69:640–651.

Terzi, E., G. Holzemann, and J. Seelig. 1994. Alzheimer beta-amyloid peptide 25–35: electrostatic interactions with phospholipid membranes. *Biochemistry.* 33:7434–7441.

Terzi, E., G. Holzemann, and J. Seelig. 1995. Self-association of beta-amyloid peptide (1–40) in solution and binding to lipid membranes. *J. Mol. Biol.* 252:633–642.

Terzi, E., G. Hölzemann, and J. Seelig. 1997. Interaction of Alzheimer beta-amyloid peptide(1–40) with lipid membranes. *Biochemistry.* 36: 14845–14852.

Vargas, J., J. M. Alarcon, and E. Rojas. 2000. Displacement currents associated with the insertion of Alzheimer disease amyloid beta-peptide into planar bilayer membranes. *Biophys. J.* 79:934–944.

Volles, M. J., and P. T. Lansbury, Jr. 2003. Zeroing in on the pathogenic form of alpha-synuclein and its mechanism of neurotoxicity in Parkinson's disease. *Biochemistry.* 42:7871–7878.

Yip, C. M., E. A. Elton, A. A. Darabie, M. R. Morrison, and J. McLaurin. 2001. Cholesterol, a modulator of membrane-associated Abeta-fibrillogenesis and neurotoxicity. *J. Mol. Biol.* 311:723–734.